Magnetic anisotropy of extended defects and vicinal surfaces of 3*d* transition metals

Ricardo Gómez-Abal and Ana María Llois
Departamento de Física, Comisión Nacional de Energía Atómica, Avenida del Libertador 8250, 1429 Buenos Aires, Argentina
(Received 26 October 2000; revised manuscript received 17 May 2001; published 5 April 2002)

The effect of linear defects and steps on the magnetocrystalline anisotropy energy of ultrathin films of Co and Fe is self-consistently calculated using an electronic tight-binding theory. The presence of linear defects produces changes in the spontaneous orientation of the magnetic moments and the induced magnetic anisotropy depends, among others, on the relative orientation of the introduced defects with respect to the substrate. A variety of possible situations is also obtained as a function of orientation index in the case of vicinal surfaces. Within our theoretical framework we obtain results that agree well with experiments.

DOI: 10.1103/PhysRevB.65.155426 PACS number(s): 73.21.−b

I. INTRODUCTION

In recent years the interest in the study of low-dimensional magnetic systems has given rise to intensive research in the field of nanoscale quantum structures. Thanks to the advances achieved in thin-film technology and atom-manipulation techniques it is possible nowadays to grow metallic films on stepped surfaces and to confine electrons on atomic scale decorated surfaces. All this has made it possible to artificially control induced surface magnetic manifestations.

The reduction of symmetry in the above-mentioned systems leads to magnetic surface anisotropies that originate from different contributions, as for instance from spin-orbit interaction (SOI).[1] Magnetocrystalline anisotropy is sensitive to the symmetry of the lattice. Atomic steps and different surface decorations locally break the rotational symmetry of the surface of an oriented single crystal and can induce uniaxial magnetic anisotropy within the film plane. One of the difficulties faced by the theoretical study of magnetic anisotropy is that the difference in energy between different spin orientations is very small (of the order or 1 μeV for bulk systems and 1 meV in surfaces and interfaces). In spite of this, many theoretical approaches to the calculation of the magnetocrystalline anisotropy energy (MAE) have appeared since the pioneering work of Gay and Richter.[2,3] The magnetocrystalline anisotropy of fcc Ni, fcc Co, and bcc Fe (001) ultrathin films has been studied by Cinal *et al.* using a perturbative tight-binding model to second order in the SOI constant.[4] Calculations using the full potential linearized plane waves method performed by Wang, Wu, and Freeman predict perpendicular orientation of the magnetic moments for Fe monolayers, and in-plane magnetization for Co monolayers,[5,6] while Szunyogh *et al.* have calculated the MAE for thin films of Fe and Co deposited on Au, using a relativistic spin-polarized screened Korringa-Kohn-Rostoker method.[7–9] In a recent contribution we have systematically studied the behavior of MAE in 4*d* transition-metal monolayers deposited on bcc Fe (001) and have shown that the sign of the SOI contribution to MAE is not only determined by band features lying near de Fermi level but also by those coming from energy bands lying well below it.[10]

As it is well known, symmetry and dimensionality play an important role in determining the MAE of transition-metal systems. Several groups have fabricated metallic films on stepped surfaces and the step induced anisotropy has been observed in different magnetic overlayer systems, such as Co/Cu (001),[11,12] Fe/W (100),[13] Fe/Ag (100),[14] and Fe films on a curved Ag (001) substrate.[14] In the case of Co, a linear dependence of the MAE as a function of the angle was observed, while for Fe this dependence was found to be quadratic. Till now, the theoretical treatments of uniaxial in-plane MAE at step edges and decorated surfaces have been mainly done within micromagnetic models, either using nearest- neighbor exchange interactions with parameters obtained from *ab initio* calculations for films of variable thicknesses,[15,16] or by considering the change in the dipolar energy due to a modulation in the surface profile.[17] To our knowledge, exceptions to this kind of treatment are those of Drùzinic and Hübner[18] and Dorantes-Dávila and Pastor.[19] Drùzinic and Hübner calculated recently the MAE for free-standing chains and rings of Fe using an electronic tight-binding Hamiltonian with *d* orbitals and doing a nonperturbative treatment of the spin-orbit interaction term. Dorantes-Dávila and Pastor also calculated recently the MAE of 3*d* transition metal wires as a function of length, width, and *d*-band filling and also for Co wires deposited on Pd (110) by doing self-consistent calculations with a *d*-band tight-binding Hamiltonian and showed that ladders and deposited chains present important in-plane anisotropies.

In this work we calculate the contribution to MAE induced by lines of atoms deposited on Co and Fe free-standing (001) monolayers and also by periodically stepped monolayers of the same materials. We are interested in the dependence of MAE on defect orientation and on surface index in the case of vicinal surfaces. We obtain this contribution directly from the calculation of the electronic structure without resorting to phenomenological models. We include the SOI completely nonperturbatively.

This paper is organized as follows. In Sec. II we give a brief description of the method of calculation. In Sec. III A we show some results obtained for the MAE of Fe and Co thin films and for the orbital magnetic moments of the bulk and thin films of the same materials and compare them with other already existing data in the literature. In Secs. III B and III C we show the results obtained for deposited lines and stepped monolayers of Fe and Co. Finally, in Sec. IV we conclude.

TABLE I. Spin-orbit coupling parameter in eV units.

	Fe	Co
p	0.0158	0.0173
d	0.065	0.0818

II. CALCULATION DETAILS

We use a periodic *spd* tight-binding Hubbard Hamiltonian solved in the unrestricted Hartree-Fock approximation and parametrize it as in previous works[10,20,21] After obtaining a self-consistent solution for the Hubbard Hamiltonian H_{TB} we construct the Hamiltonian;

$$H_\alpha = H_{TB} + H_{so}^\alpha . \tag{1}$$

H_{so}^α is the spin-orbit term, with α being the spin-quantization axis. This term is of the form

$$H_{so} = \xi \hat{L} \cdot \hat{S}, \tag{2}$$

where ξ is the spin-orbit interaction parameter for which we use the values given by Herman-Skillman (See Table I) for *p* and *d* orbitals. With this new Hamiltonian we perform one further diagonalization of H_α for the different spin quantization axes. The expression of the $\hat{L} \cdot \hat{S}$ operator matrix elements as a function of the spherical coordinates of the spin-quantization axis for Slater-Koster *d* orbitals can be found in Ref. 22.

To calculate the SOI contribution to the MAE we use the so-called ''force theorem,'' whose validity for magnetocrystalline anisotropy in surfaces and interfaces has been rigorously proven by Wang *et al.*[23] According to it, the magnetocrystalline anisotropy energy is given by the difference in band energies between two orientation directions.

$$\Delta E_{so} = E_{band}^{\perp} - E_{band}^{\parallel}, \tag{3}$$

where

$$E_{band}^{\alpha} = \sum_{i,n}^{occup} \int_{BZ} \varepsilon_{in}^{\alpha}(\vec{k}) d\vec{k}, \tag{4}$$

$\varepsilon_{in}^{\alpha}(\vec{k})$ are the eigenvalues of H_α, *i* indicates the atom in the cell, and *n* is the band index. Besides SOI, there is another contribution to MAE coming from the magnetostatic dipole-dipole interaction, this term is given by

$$E_{dd} = \frac{1}{c^2} \sum_{i \cdot j} \frac{1}{|\vec{R}_i - \vec{R}_j|^3} \times \left(\vec{\mu}_i \cdot \vec{\mu}_j - 3 \frac{[\vec{\mu}_i \cdot (\vec{R}_i - \vec{R}_j)][\vec{\mu}_j \cdot (\vec{R}_i - \vec{R}_j)]}{|\vec{R}_i - \vec{R}_j|^2} \right), \tag{5}$$

where $\vec{\mu}_i$ is the total magnetic moment of the atom in site *i*, that is, the sum of the spin and orbital magnetic moments.

For ferromagnetic systems, this expression can be reduced to

$$E_{dd} = \sum_{ij} \mu_i \mu_j \hat{n} \cdot \mathbf{M}_{ij} \cdot \hat{n}, \tag{6}$$

where $\mathbf{M}_{ij}$ is a tensor of rank 2, consisting of a Madelung like summation defined by

$$\mathbf{M}_{ij} = \frac{1}{c^2} \sum_{\vec{R}_\parallel}{}' \frac{1}{|\vec{R}_\parallel + \vec{R}_i - \vec{R}_j|^3} \times \left[\mathbf{I} - 3 \frac{(\vec{R}_\parallel + \vec{R}_i - \vec{R}_j) \otimes (\vec{R}_\parallel + \vec{R}_i - \vec{R}_j)}{|\vec{R}_\parallel + \vec{R}_i - \vec{R}_j|^2} \right], \tag{7}$$

where $\vec{R}_\parallel$ is a vector of the two-dimensional Bravais lattice and $\vec{R}_i$ and $\vec{R}_j$ are the positions of the atoms in the cell. **I** is the 3×3 identity matrix and $\otimes$ is the external vector product. The primed sum indicates that the term for which the denominator vanishes is excluded. Taking into account the results obtained for different orientations of the spin we have $\Delta E_{dd} = E_{dd}^{\perp} - E_{dd}^{\parallel}$. And the magnetic anisotropy energy is given by ;

$$\mathrm{MAE} = \Delta E_{so} + \Delta E_{dd} \tag{8}$$

The values of the SOI contribution to MAE being very small, typically of the order of 1 meV, it is necessary to use a very dense mesh for the $\vec{k}$ space integration. We use a set of special points taken from Ref. 24. As some of the symmetries of the Bravais lattice are broken in the presence of SOI we use a quarter of the Brillouin Zone (BZ) for the integration when the spin quantization axis points perpendicular to the surface, and half of it in the case of in-plane orientation of the magnetic moments. The values of MAE are already well converged for 1024 $\vec{k}$ points in the whole BZ, but in order to completely ensure convergence we use a mesh corresponding to 4096 $\vec{k}$ points in the whole BZ in all the calculations of this work.

III. RESULTS

A. Bulk and thin (001) Fe and Co films

To check the precision of our method we compare values obtained for spin and orbital magnetic moments, μ_{spin} and $\mu_{orbital}$, respectively, of bulk Fe and Co with those from other calculations[25–28] and with experimental data. See Table II. The accuracy achieved is comparable to that of the other calculations.

In Table III we show the values obtained for the different contributions to MAE of Fe and Co (001) monolayers. They agree qualitatively well with previous works.[3,5,7,29,30] The sign of MAE, and the orientation of the magnetic moments is determined in the case of monolayers by the SOI. In Table IV we show the values obtained for μ_{spin} and $\mu_{orbital}$ for the same monolayers, together with those existing in the literature.

TABLE II. Orbital and spin magnetic moments of bulk materials in μ_B units.

	μ_{spin}			$\mu_{orbital}$		
	This work	Other calc.	Experimental	This work	Other calc.	Experimental
Fe (bcc)	2.09	2.21 [a]		0.07	0.06 [a]	0.08 [a, b]
		2.13 [b]	2.13 [a, b]		0.07 [b]	
		2.16 [c]			0.05 [c]	
		2.19 [d]			0.08 [d]	
Co (fcc)	1.68	1.60 [a]		0.085	0.12 [a]	0.14 [a, e]
		1.57 [c]	1.52 [a, e]		0.08 [c]	
		1.62 [d]			0.12 [d]	

[a]Reference[25].
[b]Reference[26].
[c]Reference[27].
[d]Reference[28].
[e]hcp structure.

In Fig. 1 we show the MAE for Fe (bcc) and Co (fcc) thin films grown in the (001) direction as a function of growing number of layers. For Fe films the transition from perpendicular to in-plane orientation occurs between one and two layers, in qualitative agreement with the experimental observations.[31–33] In the case of thin Co films the SOI contribution to MAE (not shown) favors the in-plane magnetization for some thicknesses and the perpendicular orientation for others, but the magnetostatic dipole-dipole interaction is large enough to prevent a reorientation of the magnetic moments, the in-plane orientation always being the preferred one. In both materials, the dipolar interaction will dominate when the number of layers gets larger, since SOI is a surface term. Consequently, for thicker layers the preferred orientation will be in plane, and the dependence of MAE on the number of layers will be almost linear. These results are in agreement with the experimental ones for Co layers grown on Cu as reported by Krams *et al.*,[34] and with other calculations. Since we are not including the substrate in our calculations, the agreement of our results with experiments means that the orientation of the moments on the studied surfaces is a property of the Fe surface layer that is not modified by the substrate used in the experiments. This statement holds for all the comparisons with experimental results done in this paper.

TABLE III. Different contributions to MAE ($\Delta E = E_\perp - E_\parallel$) for Fe and Co (001) monolayers in meV units. The values obtained from other authors include the SOI contribution only.

	Fe	Co
This work (ΔE_{dd})	0.30	0.22
This work (ΔE_{so})	−0.54	1.1
Ref. 3	−0.4	
Ref. 7	−0.6	
Ref. 5		1.35
Ref. 4	−5.5	3.38
Ref. 38	−0.41	
Ref. 29		4.03
Ref. 30	−2.17	

B. Deposited lines

The calculations are done for lines of adatoms deposited on both sides of a (001) free-standing monolayer of the same kind of atoms as the adsorbed lines, see Fig. 2. The interatomic distances in all cases are those corresponding to the respective bulk materials.

In Fig. 3(a) we show the MAE per surface atom for the case of Fe like occupation as a function of the distance between lines when these are grown along the (100) direction. The spontaneous orientation of the moments changes from parallel to perpendicular to the monolayer with growing distance between adsorbed lines. This behavior is due to the fact that for short distances this system can be considered as being a trilayer for which the moments are in-plane oriented, while for large defect separations it approaches the monolayer for which the perpendicular orientation is the preferred one (see Fig. 1). The adsorbed lines give rise to a breaking of the surface fourfold symmetry and within the plane the preferred orientation of the magnetic moments oscillates from parallel to perpendicular to the chains as a function of the distance between them. Figure 3(b) shows the same as Fig. 3(a) but for Fe lines grown along the (110) direction. The spontaneous orientation is again perpendicular to the monolayer for large distances between lines, but parallel for small ones, as in the previous case. The in-plane magnetic anisotropy would always favor an orientation of the magnetic mo-

TABLE IV. Orbital and spin magnetic moments of the monolayers in μ_B units.

		Fe	Co
$\mu_{orbital}$	This work	0.075	0.12
	Ref. 7	0.125	
	Ref. 39	0.094	
μ_{spin}	This work	3.03	2.08
	Ref. 7	3.15	
	Ref. 38	3.3	
	Ref. 30	2.95	
	Ref. 39	3.05	

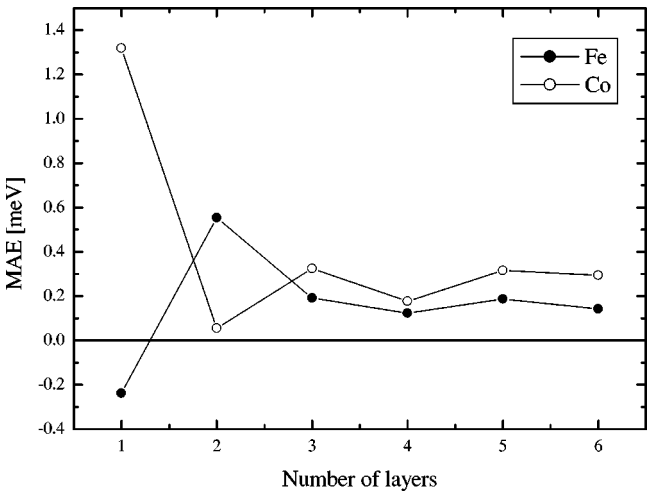

FIG. 1. Magnetocrystalline anisotropy energy per atom as a function of the number of layers for Fe (●) and Co (○) thin films grown in the (001) direction.

ments parallel to the lines. The uniaxial in-plane anisotropy clearly depends upon the orientation of the chains with respect to the substrate.

The case of Co is even more interesting since the anisotropy is always in-plane, so that the uniaxial in-plane magnetic anisotropy always determines the spontaneous orientation of the magnetic moments. In Fig. 4(a) we show the MAE as a function of the distance between chains when these are grown along the (100) direction. The preferred orientation changes from perpendicular to parallel to the defects when the distance between them goes from two to three lattice parameters. In Fig. 4(b) we show the results for chains grown along the (110) direction, the preferred orientation presents in this case the opposite behavior, that is, it goes from parallel to perpendicular to the defects as the distance between them grows. We are making in all cases the simplifying assumption that all spins point in the same direction.

The in-plane magnetic anisotropy energy $(E_y - E_x)$ should go to zero for large distances in between the lines.

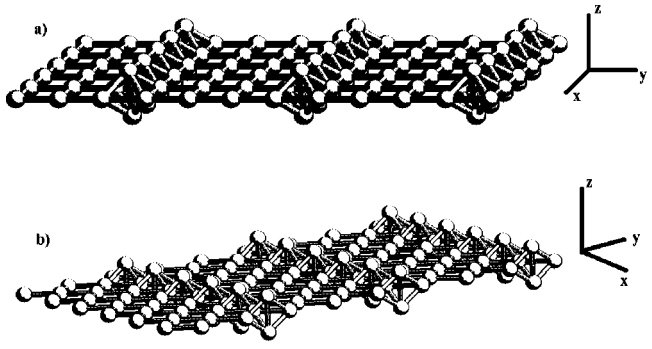

FIG. 2. Fe lines deposited on a Fe-bcc(001) monolayer in the (a) (100) and (b) (110) direction. It has to be taken into account that in the case of Co the indexes are exchanged due to the fcc structure considered.

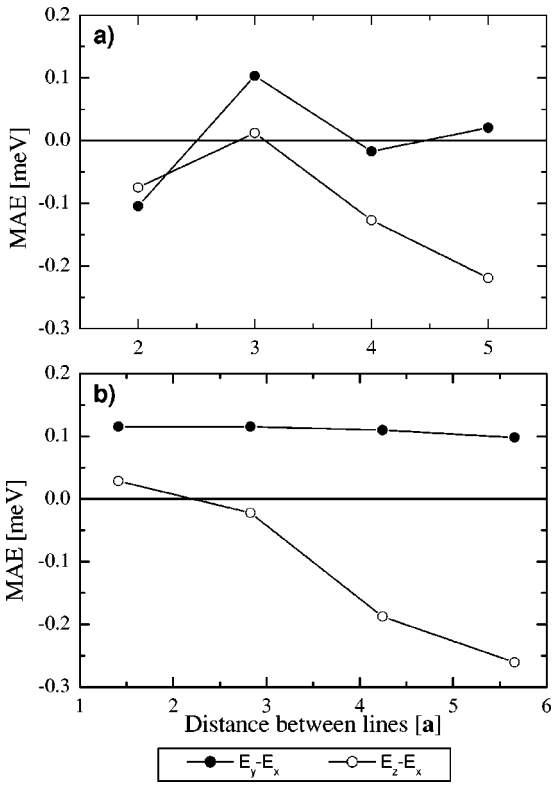

FIG. 3. Magnetocrystalline anisotropy energy per atom for Fe lines grown in the (a) (100) and (b) (110) direction. The subscripts *x*, *y*, and *z* correspond to the magnetic moments aligned in the corresponding direction as shown in Fig. 2 . The distance between lines is given in units of the the surface lattice parameter.

The range of distances covered by our calculations (Figs. 3 and 4) are too small to show such a tendency.

C. Stepped monolayers

The steplike structures for which we calculate MAE are those of Fig. 5. In Fig. 6(a) we show the MAE for Fe monolayers of [01*N*] indexes as a function of the angle formed with the (001) direction. It can be seen that a reorientation transition takes place around 15°. For smaller angles, that is, for monolayer growth directions close to the (001), the favored orientation of the magnetic moments is the perpendicular one while for larger angles the moments prefer to align parallel to the steps. The in-plane MAE always favors the orientation of the moments parallel to the steps. This result agrees with the experimental ones obtained for angles smaller than 10° for the case of Fe deposited on Ag (001).[35]

In the case of Fe monolayers of [11*N*] indexes the parallel to perpendicular transition takes place for very small angles (less than 4°), as it can be seen in Fig. 6(b). The dipole-dipole energy dominates and the preferred direction is in-plane and parallel to the steps for nearly the whole range of angles considered. The value of the dipole-dipole energy we obtain is of the same order of magnitude as the one given in Ref. 17 extrapolating the data to zero applied magnetic field.

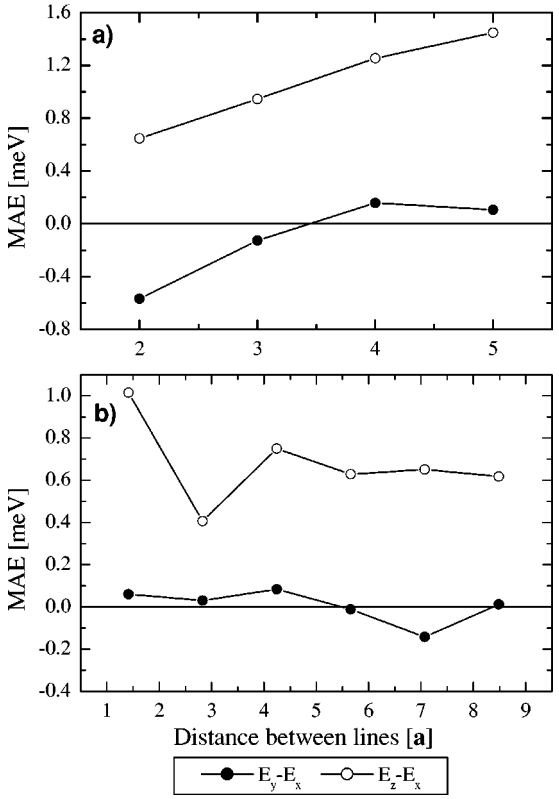

FIG. 4. Magnetocrystalline anisotropy energy per atom for Co lines grown in the (a) (100) and (b) (110) direction. The subscripts *x*, *y*, and *z* correspond to the magnetic moments aligned in the corresponding direction as shown in Fig. 2. The distance between lines is given in units of the surface lattice parameter.

In Fig. 7(a) the MAE for Co monolayers with $[01N]$ indexes is shown as a function of the angle with the (001) monolayer. In this case no transition is observed, the preferred orientation is always in plane and perpendicular to the steps. For $[11N]$ indexes the situation is more interesting, the orientation has a tendency to be perpendicular to the steps for angles smaller than 6° and it is clearly parallel for larger ones. As in the case of the ideal (001) Co monolayer, the spontaneous magnetic orientation is never perpendicular to

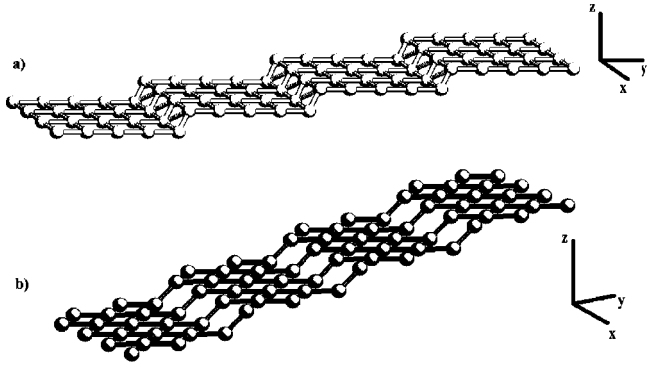

FIG. 5. Fe monolayers vicinal to the Fe-bcc(001) monolayer, with indexes (a) [0,1,10] and (b) [1,1,10]. It has to be taken into account that in the case of Co the indexes are exchanged, since it has fcc structure.

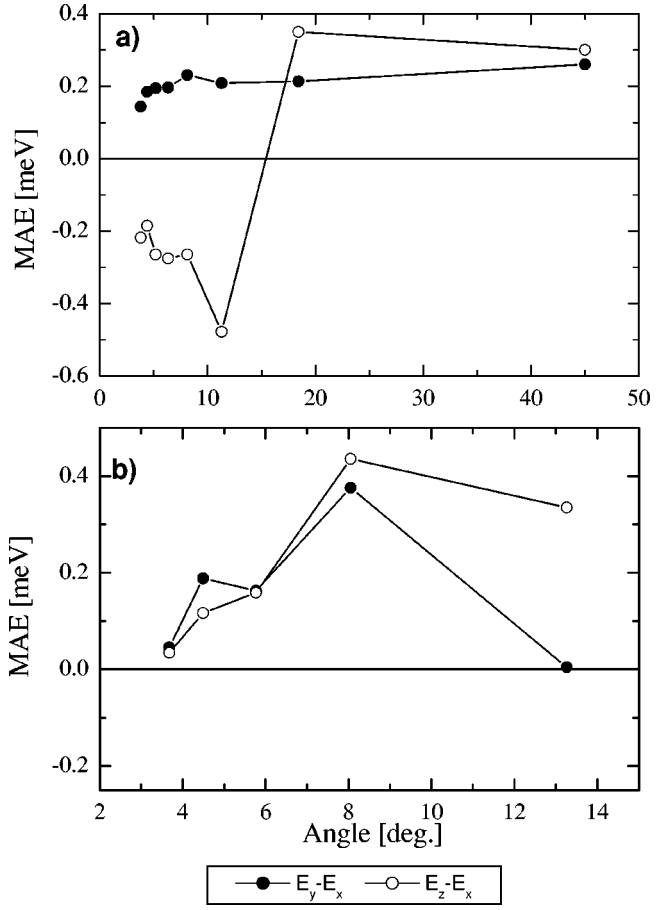

FIG. 6. Magnetocrystalline anisotropy energy per atom for Fe (a) $[01N]$ and (b) $[11N]$ monolayers as a function of the angle between them and the (001) monolayer. The subscripts *x*, *y*, and *z* correspond to the magnetic moments aligned in the corresponding direction as shown in Fig. 5.

it. Contrary to what happens for Fe vicinal surfaces, the uniaxial in-plane anisotropy depends in the case of Co upon the orientation of the steps.

Experimental results for thin Co $[11N]$ films and angles smaller than 6°, show an orientation of the magnetic moments that is parallel to the steps for thicknesses going from 4 to 15 monolayers.[12,35–37] Extrapolation of the anisotropy energy for smaler thicknesses, made by Krams *et al.*,[35] predicts a change of sign in the MAE for films of less than three monolayers, in agreement with our results. Even if the number of values we have calculated in the range betwwen 0° and 8° is small, the MAE does not seem to follow the linear (quadratic) behavior experimentally observed in Co (Fe) thin films.[12–14] This discrepancy could be due to substrate, thickness, or strain effects, which are not being considered in our calculations.

Another interesting data obtained from the eigenvectors calculated after including the SOI in the Hamiltonian are the orbital moments. In order to follow the general trends we have selected some particular examples for which we give the values of the orbital moments. In the presence of linear defects the lowest values of the orbital moment correspond to the atoms lying closest to the adsorbed lines, while the

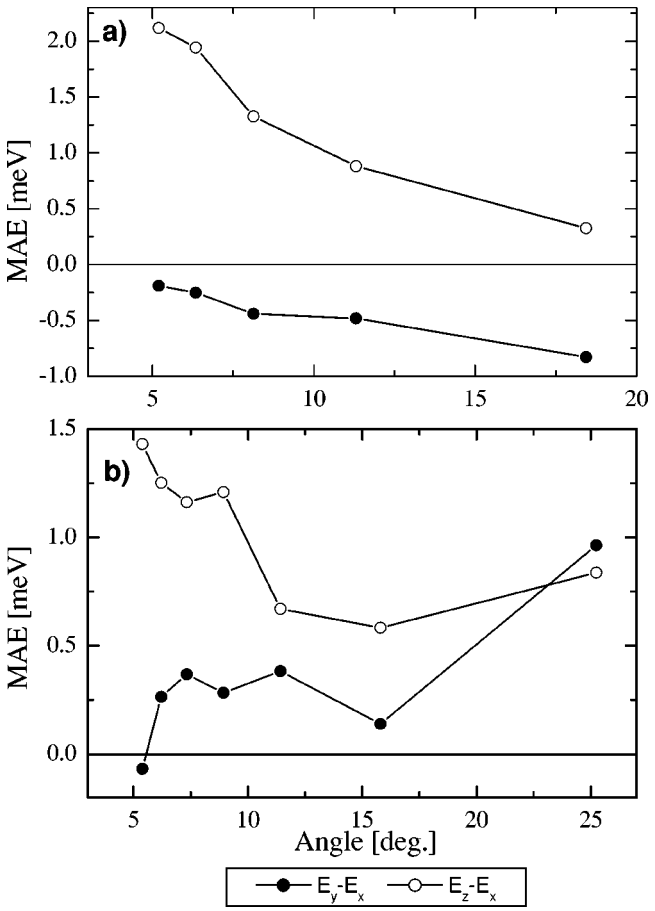

FIG. 7. Magnetocrystalline anisotropy energy per atom for Co (a) $(01N)$ and (b) $(11N)$ monolayers as a function of the angle between them and the (001) monolayer. The subscripts *x*, *y*, and *z* correspond to the magnetic moments aligned in the corresponding direction as shown in Fig. 5.

largest ones correspond to those atoms lying midway in between them. The reason for this behavior is that in a monolayer the last kind of atoms are the less coordinated ones. In other words, the larger the coordination the lower the orbital moment. A similar behavior is obtained for the stepped surfaces. In Table V we give the results for Fe. In the presence of a surface, that is a semi-infinite crystal, the atoms on the deposited lines or at the step edges should be the ones with the largest orbital moments.

IV. CONCLUSIONS

We have shown that a large variety of magnetic structures can be induced by decorating Fe and Co thin films with surface defects. The presence of linear defects on Fe monolayers gives rise to a change in the spontaneous direction of the magnetization. This anisotropy depends upon the orientation of the linear defects with respect to the underlying surface as well as on defect density.

In the case of surfaces vicinal to the (001) Fe monolayer, the magnetic moments end up being perpendicular to the surface for small angles and in plane for larger ones. The angle for which the transition occurs depends on the orientation of the steps with respect to the (001) direction. Once the transition has taken place the in-plane orientation is always parallel to the steps for the studied cases.

In the case of Co, the orientation of the magnetic moments is always in plane for the (001) monolayer but the in-plane anisotropy in the case of linear defects depends upon orientation and density of the defects. In Co monolayers vicinal to the (001) direction, the magnetic moments align perpendicular to the steps for monolayers of index $[01N]$, while for $[11N]$ indexes the spontaneous orientation is perpendicular to the steps for angles smaller than 6° (in agreement with experimental results) and parallel to them for larger angles.

With respect to the values of the orbital moments we obtain, as expected that they grow with decreasing atomic coordination.

The variety of results obtained is due to the fact that MAE is not only a symmetry property, but a combination of symmetry effects, band filling, and interaction intensity, the latter

TABLE V. Orbital magnetic moments for the case of linear defects deposited on Fe monolayers and for Fe [018] vicinal surfaces, in μ_B units. Adsorbed Fe lines: "1" stands for adsorbed atoms, "2" stands for atoms closer to the adsorbed lines [lines along the (100) direction] or for atoms just below the adsorbed lines [lines along (110) direction], "3" stands for atoms lying midway inbetween lines [defects along (100)] or atoms closer to adsorbed lines [defects along (110)], "4" stands for atoms midway in between adsorbed lines [defects along (110)]. Fe [018] vicinal surface: "1" means atom at the step edge, "2" atom in the center of a step.

	Fe lines deposited in the (100) direction (distance $=3a$)			
Atom	1	2	3	
$\mu_{orbital}(\mu_{spin})$	0.094(3.24)	0.082(3.19)	0.109(3.38)	
	Fe lines deposited in the (110) direction (distance $=2.82a$)			
Atom	1	2	3	4
$\mu_{orbital}(\mu_{spin})$	0.134(3.00)	0.078(3.07)	0.116(3.15)	0.156(3.37)
	Fe [018] vicinal surface (Angle $=11.3°$)			
Atom	1		2	
$\mu_{orbital}(\mu_{spin})$	0.147(3.04)		0.169(3.18)	

being strongly material dependent. We have shown that we can reliably predict and thereafter, in principle, induce the desired magnetic anisotropy by the proper selection of the low-dimensional defects to be used to decorate a surface, this can be inferred from the good agreement obtained in those cases where the comparison with experiments is feasible.

ACKNOWLEDGMENTS

We acknowledge the Consejo Nacional de Investigaciones Científicas y Técnicas (CONICET), SECyT (Grant PICT 03-00105-02043), and UBACyT (TW19) of Argentina for partial support.

[1] D.S. Wang, R. Wu, and A.J. Freeman, Phys. Rev. Lett. **70**, 869 (1993), and references therein.
[2] J.G. Gay and R. Richter, Phys. Rev. Lett. **56**, 2728 (1986).
[3] J.G. Gay and R. Richter, J. Appl. Phys. **61**, 3362 (1987).
[4] M. Cinal, D.M. Edwards, and J. Mathon, Phys. Rev. B **50**, 3754 (1994).
[5] D.S. Wang, R. Wu, and A.J. Freeman, Phys. Rev. B **48**, 15 886 (1993).
[6] D.S. Wang, R. Wu, and A.J. Freeman, Phys. Rev. B **47**, 14 932 (1993).
[7] L. Szunyogh, B. Újfalussy, and P. Weinberger, Phys. Rev. B **51**, 9552 (1995).
[8] L. Szunyogh, B. Újfalussy, and P. Weinberger, Phys. Rev. B **55**, 14 392 (1997).
[9] L. Szunyogh, B. Újfalussy, P. Bruno, and P. Weinberger, J. Magn. Magn. Mater. **165**, 254 (1997).
[10] R. Gómez-Abal and A. M. Llois, Phys. Rev. B **60**, 12 841 (1999).
[11] W. Weber, C.H. Back, A. Bischof, Ch. Würsch, and R. Allenspach, Phys. Rev. Lett. **76**, 1940 (1996).
[12] R.K. Kawakami, M.O. Bowen, H.J. Choi, E.J. Escorcia-Aparicio, and Z.Q. Qiu, Phys. Rev. B **58**, R5924 (1998).
[13] H.J. Choi, Z.Q. Qiu, J. Pearson, J.S. Jiang, D. Li, and S.D. Bader, Phys. Rev. B **57**, R12 713 (1998).
[14] R.K. Kawakami, E.J. Escorcia-Aparicio, and Z.Q. Qiu, Phys. Rev. Lett. **77**, 2570 (1996).
[15] A.B. Shick, Y.N. Gornostirev, and A.J. Freeman, Phys. Rev. B **60**, 3029 (1999).
[16] R.A. Hyman, A. Zangwill, and M.D. Stiles, Phys. Rev. B **58**, 9276 (1998).
[17] R. Arias and D.L. Mills, Phys. Rev. B **59**, 11 871 (1999).
[18] R. Drŭzinic and W. Hübner, Phys. Rev. B **55**, 347 (1997).
[19] J. Dorantes-Dávila and G.M. Pastor, Phys. Rev. Lett. **81**, 208 (1998).
[20] R. Gómez Abal, A.M. Llois, and M. Weissmann, J. Phys.: Condens. Matter **8**, 6607 (1996).
[21] G. Fabricius, A.M. Llois, M. Weissmann, and M.A. Kahn, Phys. Rev. B **49**, 2121 (1994).
[22] H. Takayama, K. Bohnen, and P. Fulde, Phys. Rev. B **14**, 2287 (1976).
[23] X. Wang, D. Wang, R. Wu, and A.J. Freeman, J. Magn. Magn. Mater. **159**, 337 (1996).
[24] S.L. Cunningham, Phys. Rev. B **10**, 4988 (1974).
[25] O. Eriksson, B. Johansson, R.C. Albers, A.M. Boring, and M.S.S. Brooks, Phys. Rev. B **42**, 2707 (1990).
[26] J. Igarashi and K. Hirai, Phys. Rev. B **50**, 17 820 (1994).
[27] G.H.O. Daalderop, P.J. Kelly, and M.F.H. Schuurmans, Phys. Rev. B **41**, 11 919 (1990).
[28] J. Trygg, B. Johansson, O. Erikson, and J.M. Wills, Phys. Rev. Lett. **75**, 2871 (1995).
[29] K. Kyuno, J.G. Ha, R. Yamamoto, and S. Asano, Phys. Rev. B **54**, 1092 (1996).
[30] R. Lorenz and J. Hafner, Phys. Rev. B **54**, 15 937 (1996).
[31] B.T. Jonker, K.H. Walker, E. Kisker, G.A. Prinz, and C. Carbone, Phys. Rev. Lett. **57**, 142 (1986).
[32] J. Araya-Pochet, C.A. Ballentine, and J.L. Erskine, Phys. Rev. B **38**, 7846 (1988).
[33] D.P. Pappas, C.R. Brundle, and H. Hopster, Phys. Rev. B **45**, 8169 (1992).
[34] P. Krams, F. Lauks, R.L. Stamps, B. Hillebrands, and G. Güntherodt, Phys. Rev. Lett. **69**, 3674 (1992).
[35] P. Krams, B. Hilldebrands, G. Güntherodt, and H.P. Oespen, Phys. Rev. B **49**, 3633 (1994).
[36] A. Berger, U. Linke, and H.P. Oepen, Phys. Rev. Lett. **68**, 839 (1992).
[37] D.S. Chuang, C.A. Ballentine and R.C. O'Handley, Phys. Rev. B **49**, 15 084 (1994).
[38] A. Lessard, T.H. Moos, and W. Hübner, Phys. Rev. B **56**, 2594 (1997).
[39] G.Y. Guo, W.M. Temmerman, and H. Ebert. J. Phys.: Condens. Matter **3**, 8205 (1991).